Heliyon 10 (2024) e25433

Contents lists available at ScienceDirect

Heliyon

journal homepage: www.cell.com/heliyon

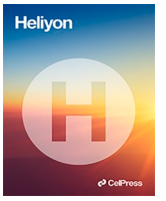

Research article

Photocatalytic degradation of ciprofloxacin from water with waste polystyrene and TiO_2 composites

Tugba Hayri-Senel *, Ebru Kahraman, Serhat Sezer, Nalan Erdol-Aydin, Gulhayat Nasun-Saygili

Istanbul Technical University, Faculty of Chemical and Metallurgical Engineering, Department of Chemical Engineering, Turkey

A B S T R A C T

Ciprofloxacin (CIP) is one of the widely used antibiotics with a broad antimicrobial spectrum in the fluoroquinolone type. Its concentration in water bodies has increased over the years due to its frequent use. Since ciprofloxacin in the aquatic ecosystem adversely affects human health as well as other organisms, it must be removed from wastewater.

The aim of this study was to develop Polystyrene (PS) and Titanium dioxide (TiO_2) composites that can be used as catalysts in CIP removal by photocatalytic process. Waste PS (obtained from disposable cutlery) was used in the synthesis of these composites. In this study, PS-TiO_2 composites with different PS content (C20, C50, C80; the numbers in the names indicate the PS percentage in the composite by weight) were synthesized. This is important in terms of the use of one waste in the removal of another waste.

This process was optimized using Box-Behnken design, one of the response surface method. Parameters such as the amount of polymer in the composite, pH and initial CIP concentration were studied and their effects on CIP removal were found. The validity and adequacy of the selected model were evaluated according to the relevant statistical data. These are $R^2 = 0.9751$, adjusted $R^2 = 0.9565$, the model's p-value <0.05 and the lack of fit-value 0.246. Optimum conditions for CIP removal were obtained when the C50 was used, with a pH value of 3 and an initial CIP concentration of 5 mg/L.

In the process carried out under these conditions, the CIP removal was found to be 95.01 % at the end of 180 min. This value was predicted as 94.37 % in the model. According to these results, C50 composite synthesized with waste PS can be used effectively for CIP removal.

1. Introduction

Ciprofloxacin (CIP) is a fluoroquinolone antibiotic with a broad antimicrobial spectrum. CIP is one of the most widely used antibiotics for both humans and animals. It can be used for many diseases such as digestive and urinary tract infections, various skin and lung diseases [1,2].

Over the years, the concentration of antibiotics in water bodies has increased. Ciprofloxacin concentration varies according to sources. In the literature, there are studies showing that the concentration of CIP in wastewater treatment plants, raw drinking water, hospital wastewater, lakes, and discharges of the pharmaceutical industry has been reported as 11–99, 0.032, 150, 6.5 and 31–50 mg/L, respectively [1].

CIP in the aquatic ecosystem adversely affects human health as well as other organisms there. In addition, ciprofloxacin in the environment leads to the formation of antibiotic-resistant bacteria, resulting in higher dose antibiotic requirements in bacterial infections [3].

Considering the significant detection of ciprofloxacin in aquatic environments, the necessity of removing it from wastewater

* Corresponding author.
E-mail address: hayri16@itu.edu.tr (T. Hayri-Senel).

https://doi.org/10.1016/j.heliyon.2024.e25433
Received 9 October 2023; Received in revised form 19 January 2024; Accepted 26 January 2024
Available online 29 January 2024

emerges. In the literature, there are studies on the removal of ciprofloxacin from wastewater [2–11]. One of the most common techniques used for this purpose is the photocatalytic degradation of ciprofloxacin [1,12].

Titanium dioxide, TiO_2, is an abundant, stable, economical, efficient photocatalyst that is widely used due to its high catalytic activity, high oxidizing power, and high photocorrosion resistance. It serves many different fields, especially waste water treatment [1, 12,13].

In the photocatalytic degradation mechanism of CIP with TiO_2, firstly e^- and h^+ pairs are formed by stimulating TiO_2 under the influence of light energy **(1)**. Both reactive species participate in different reactions and contribute to the formation of (•OH) and ($\bullet O_2^-$) radicals **(2,3,4,5)**. All these reactive species and radicals (h^+, •OH, $\bullet O_2^-$) that may be present in the environment can effectively degrade CIP molecules **(6,7,8)**. Since the CIP structure contains regions suitable for attack, such as the piperazine ring, F atom, carboxyl group and cyclopropyl group, they cause different degradation pathways to be exhibited. Which possibilities will occur varies depending on the conditions of the environment, making it difficult to specify a definitive path. Studies have reported that solution pH is one of the most effective parameters in determining the photocatalytic degradation pathway, as it affects the formation rates of active species [3,14,15].

(1) $TiO_2 + hv \rightarrow h^+ + e^-$
(2) $h^+ + H_2O \rightarrow \bullet OH + H^+$
(3) $e^- + O_2 \rightarrow \bullet O_2^-$
(4) $\bullet O_2^- + H^+ + H_2O \rightarrow H_2O_2 + O_2$
(5) $H_2O_2 \rightarrow 2 \bullet OH$
(6) $h^+ + CIP \rightarrow$Degradation Products
(7) $\bullet O_2^- + CIP \rightarrow$ Degradation Products
(8) $\bullet OH + CIP \rightarrow$ Degradation Products

TiO_2 can be used in wastewater studies in powder form, or it can be used in combination with suitable substrates. When used in powder form, higher surface area and accordingly higher efficiency can be obtained. However, some problems arise when used in powder form. One of these problems is that recovery of the catalyst after application is difficult, time consuming and expensive. Also, there is a loss of catalyst at this stage. The most widely used way to overcome these disadvantages is the immobilization of TiO_2 with various substrates. Although the reaction surface area is reduced by immobilization, it is preferred because it provides advantages such as both prolonging the life of the catalyst and increasing its reusability [3,9,13,16,17].

For this purpose, different support materials can be selected. Polymeric materials are widely used support materials. Polystyrene (PS) is a support material that can be preferred due to its inert structure, ease of production, low cost and ability to float in water. Plastic waste is a worldwide environmental problem. One of the commonly encountered plastic wastes is PS waste. Disposable PS products cause serious environmental problems [16]. Although there are different techniques for recycling waste PS, it does not offer a long-term solution [18]. It is very important to use these PS wastes for the removal of pollutants in different environments [16].

Photocatalytic degradation of PS and PS-TiO_2 composite was investigated in a study by Shang et al. Although pure PS was observed to degrade more slowly than PS-TiO_2 composite, it was still reported that the degradation of PS-TiO_2 composite remained below 5 % even after continuous exposure for 24 h [18].

Various statistical and mathematical methods are used to analyze different chemical processes, to save time, to predict and simulate the conditions in this process. One of the most common methods used for this purpose is Response Surface Methodology (RSM). RSM is a mathematical tool used to design experiments in many fields such as chemical processes and to evaluate the results of these experiments, which saves time by reducing the number of experiments. RSM has two design titles, Box-Behnken Design and Central Composite Design.

RSM enables determination of optimum process conditions by examining the effects of independent variables on the process through experimental design. In addition, it develops some empirical models of the process using the experimental data obtained from the experimental design. Thus, it reveals the relationship between the parameters [10,19].

In this study, first of all, PS-TiO_2 composites were synthesized and their removal performance was examined by using them as catalysts in the photocatalytic degradation of CIP from wastewater. PS used in the synthesis of composites in the study was obtained from disposable waste PS cutlery. One of the aims of this study is to ensure the reuse of disposable waste. It is also important to make PS waste suitable for reuse after only a simple washing process, without applying a complex process that requires extra high energy and cost. If this can be achieved, a more cost-effective product is expected to be obtained compared to when TiO_2 is used alone. No study has been found in the literature on CIP removal with a material similar to the one in this study (PS–TiO_2 composite). Box-Behnken Design was chosen to analyze the degradation process of Ciprofloxacin with PS-TiO_2 composites and optimize the effective parameters. MINITAB software version 21.0 was used for experimental design.

2. Materials and methods

2.1. Materials

Waste PS was collected from used waste spoons. TiO_2 (anatase, powder 99.8 %), Ciprofloxacin, chloroform and ethanol were purchased from Merck.

2.2. Characterization

X-Ray Diffraction (XRD) analysis was performed using the PANalytical XPert Pro device for the structural evaluation of anatase TiO_2, waste PS and PS-TiO_2 composite. The samples were scanned by X-ray at a wavelength of 1.5406 Å for 2 theta ranging from 10° to 90°.

The surface morphology of waste PS and its composites with different polymer content formed with TiO_2 were determined by Scanning Electron Microscope (SEM, QUANTA FEG250 Field Emission). Elemental analysis was performed using Energy dispersive analysis of X-ray (EDAX). Waste PS, TiO_2 and PS-TiO_2 composite were analyzed by FT-IR spectrophotometer (Bruker) in the range of 650 cm^{-1} to 4000 cm^{-1}. Zeta potential measurements of the PS-TiO_2 composite were carried using Malvern Zetasizer at different pH values.

2.3. Polystyrene-TiO_2 (PS–TiO_2) composite preparation

The particles obtained by cutting the waste PS spoons were cleaned by washing with distilled water. To form the PS-TiO_2 composite, a known amount of the polymer particles and TiO_2 were placed in a beaker containing 1:8 ethanol and chloroform. This mixture was homogenized in a sonication water bath for 1 h. It was then stirred at 120 °C for 2 h. The resulting solution was poured into a glass Petri dish and kept in a fume hood for 24 h for solvent evaporation. The resulting product was washed several times with distilled water in order to remove any impurities that may be on the product, and it was dried in an oven at 50 °C for 24 h [20]. This procedure was applied for all PS-TiO_2 products (Cx) containing different ratios of polystyrene. Thus, C20, C50 and C80 composites were produced. The numbers in the names refer to the percent by weight PS in the composite.

2.4. Evaluation of photocatalytic efficiencies

The efficiency of the PS-TiO_2 photocatalysts was measured by the photocatalytic degradation of an aqueous ciprofloxacin solutions. The schematic representation of the experimental system is shown in Scheme 1. Photodegradation studies were carried out under magnetic stirring at room temperature. In these studies, two LED daylight lamps (metal halide lamp, $\lambda = 400–800$ nm) were used as the light source. Ciprofloxacin solutions were prepared at different initial concentrations (5, 10 and 15 mg/L). In a typical study, 50 ml of ciprofloxacin aqueous solution was analyzed to determine the initial CIP concentration (C_0) and 20 mg of catalyst was added. The

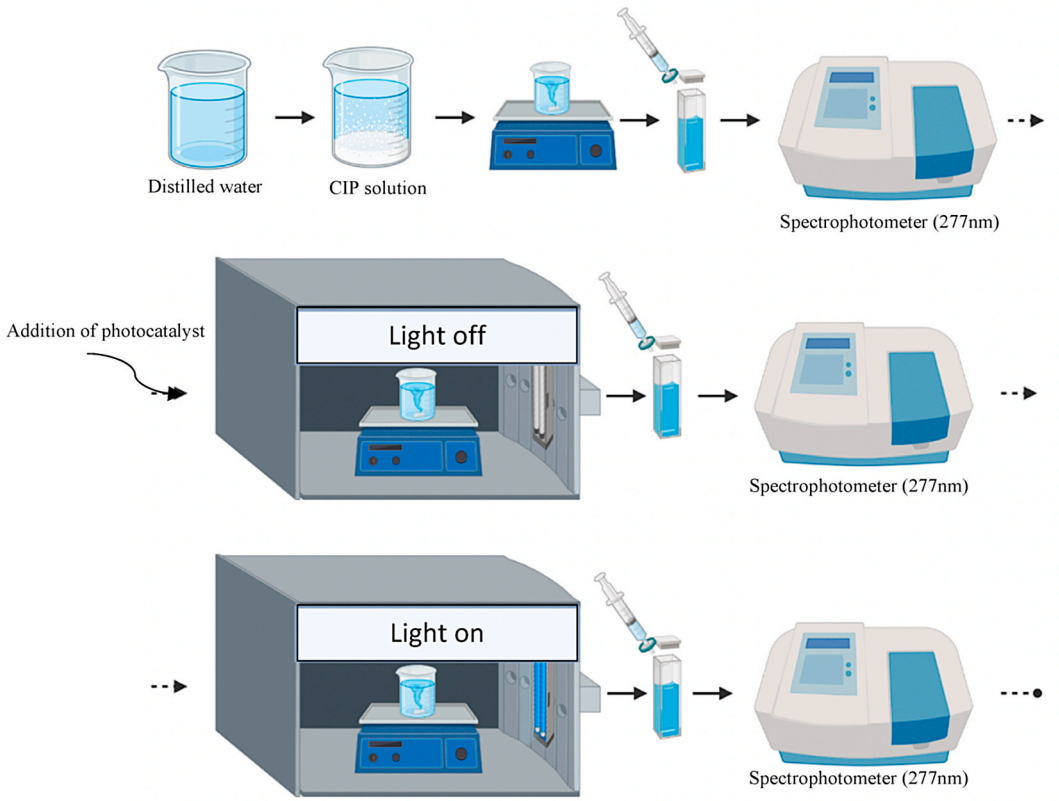

Scheme 1. The schematic representation of the experimental system.

mixture was then stirred in the dark for 30 min. Thus, the adsorption and desorption equilibrium of the mixture was achieved. At the end of this period, sample was taken from the experimental medium and analyzed. While the mixing was continuing, the LED lamps were turned on and the concentration of the samples taken from the medium were measured at certain time intervals. The samples were first filtered through a 0.20 mm PTFE membrane syringe filter and the absorbance values of the filtered solutions were determined at 277 nm with a UV–Vis spectrophotometer (Hach DR6000). The percent degradation of ciprofloxacin was calculated according to Equation (1). Here, C_0 and C_t represent the CIP concentration value at the start time (t_0) and the concentration values at any time (t), respectively.

$$Ciprofloxacin\ removal\ (\%) = \left(\frac{C_0 - C_t}{C_0}\right) x\ 100 \quad (1)$$

2.5. Experimental design

3-factor and 3-level Box-Behnken design was used to optimize ciprofloxacin removal conditions. Analysis of the results was performed with Minitab software (Minitab 21.0). The effect of three factors (independent variables) on ciprofloxacin removal was examined at three different levels, including the amount of polymer in the composite (wt%) (A), ambient pH (B), and ciprofloxacin concentration in the initial solution (C). These are presented in Table 1. The percent ciprofloxacin removal (dependent variable, Y) was determined as the response of the designed experiments. In this design used, 15 experimental studies were planned, including 3 center points. The significance of the variables was evaluated by analysis of variance (ANOVA, p-value$<$0.05), while the fit of the model was evaluated using R^2 and adjusted R^2 values. Data were fitted to obtain a quadratic polynomial. Contour charts were used to determine the effect of independent variables on dependent variables. The conditions that achieved the highest Ciprofloxacin removal were considered as optimized conditions for this system.

3. Results and discussions

3.1. XRD analysis

Fig. 1a shows the XRD pattern of anatase TiO_2. The sharp Bragg peaks indicate the highly crystalline nature of TiO_2. All characteristic peaks ($2\theta = 25.53^\circ$, 38.1°, 48.35° and 54.18°) originating from the TiO_2 anatase phase are observed [21,22]. Looking at the XRD pattern for waste PS in Fig. 1b, an amorphous polymeric structure is seen. The XRD pattern of C50 composite is also shown in Fig. 1c. This model confirms that amorphous phase is present in the compound due to PS. In addition, the broad peak at $2\theta \cong 20^\circ$ corresponds to amorphous PS. The characteristic peaks in Fig. 1a are also seen here, confirming the presence of crystalline TiO_2 in C50 [20,23].

3.2. SEM analysis

The morphologies of waste PS, C20, C50 and C80 composites were observed by SEM. SEM images are given in Fig. 2. Looking at the waste PS images in Fig. 2a and b, it is seen that it exhibits a smooth and homogeneous structure. Again, the white dots appearing in the same SEM images can be interpreted as the residual solvent (chloroform) thought to be trapped in the polymeric materials [24]. SEM images of C80, C50 and C20 show that TiO_2 is evenly distributed in the polymeric matrix [20].

3.3. EDAX analysis

Fig. 3 shows the elemental mapping results of waste PS and its composites with different PS content (C80, C50 and C20). In addition, graphs showing the elemental density of the samples are embedded in the elemental mapping results of that sample. EDAX measurements show the distribution of element C, element O and element Ti in the polymer matrix [25]. Elemental mapping results confirmed that the composite with the highest TiO_2 (C20) contained more Ti elements than the rest of the composites, as expected, depending on its content.

Table 1
Factors and levels used in Box-Behnken design.

Factors	Symbols	Levels		
		Low −1	Medium 0	High 1
Amount of polymer (in composite, % by weight)	A	20	50	80
pH	B	3	7	11
Ciprofloxacin initial concentration (mg/L)	C	5	10	15

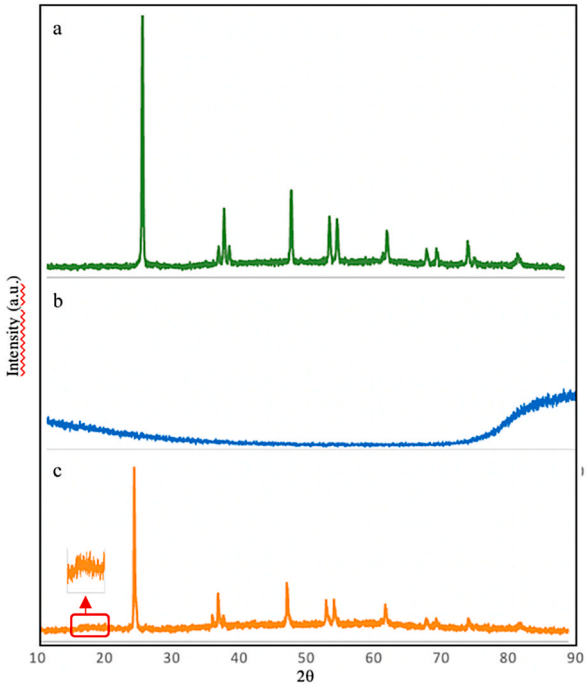

Fig. 1. The XRD patterns of a) anatase TiO_2, b) waste polystyrene, c) C50.

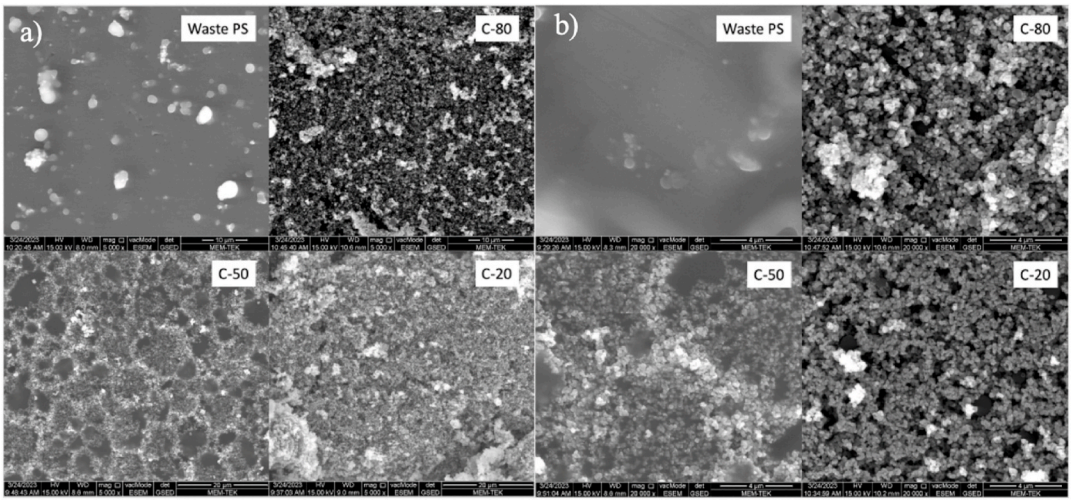

Fig. 2. SEM images of waste PS, C80, C50 and C20 a)all images for mag = 5000x b) all images for mag = 20000x.

3.4. FTIR analysis

FTIR spectra of waste PS, TiO_2 and C50 are given in Fig. 4. Looking at the IR spectra of waste PS, it is known that the peaks between 2800 and 3100 cm^{-1} originate from the C–H stretching vibration in the aromatic rings and the main chain. The peaks at 695, 748, 1027, 1451, 1492 and 1601 cm^{-1} belong to the C–H skeletal vibrations in PS [26].The peak seen in the TiO_2 curve at 721 cm^{-1} is due to the O–Ti–O bonding in the form of anatase. In addition, the peaks appearing at 1660 cm^{-1} and 3375 cm^{-1} indicate surface adsorbed water and hydroxyl groups. The fact that all characteristic peaks appearing in both waste PS and TiO_2 are also visible in the spectra of C50 shows that TiO_2 can be successfully embedded into the PS polymer matrix [27–30].

3.5. Zeta potential

Zeta potential measurements at different pH values of the C50 composite synthesized using PS and TiO_2 are given in Fig. 5. It is

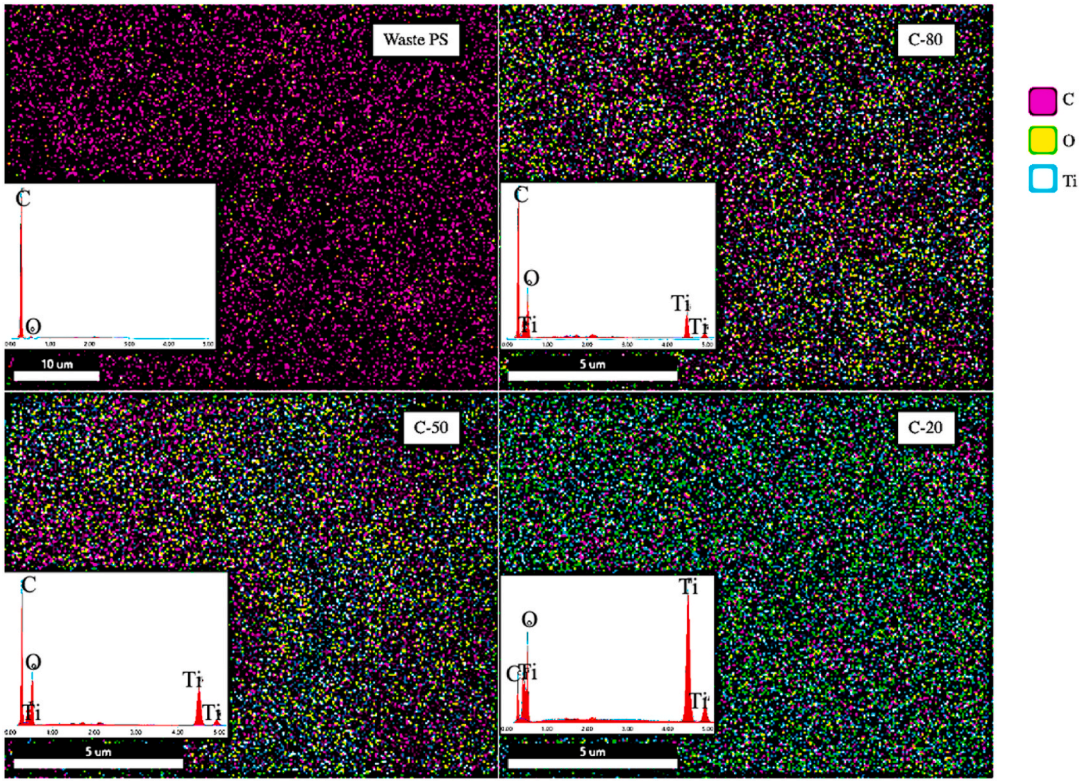

Fig. 3. EDAX mapping of waste PS, C80, C50 and C20.

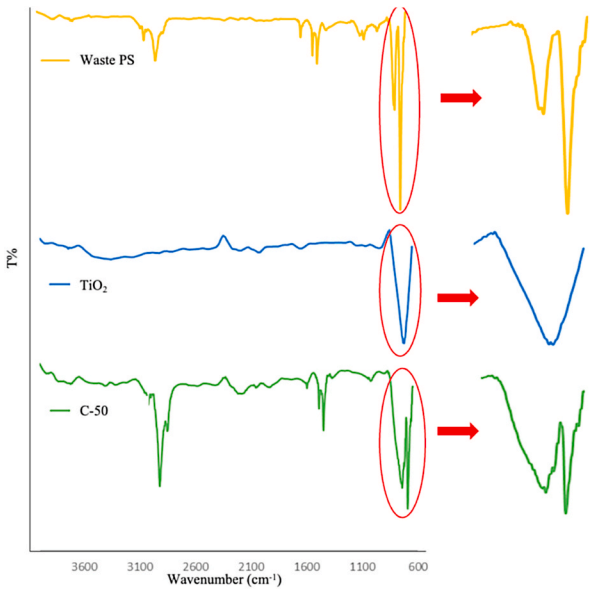

Fig. 4. FTIR spectra of waste PS, TiO_2 and C50.

known that CIP exists in different ionic forms at different pHs. In addition to this behavior of CIP, knowing the behavior of the synthesized composite at different pHs plays an important role in better understanding the interaction between them and explaining the removal process. In order to examine this important effect of pH on removal performance in more depth, it was desired to benefit from zeta potential values. For this reason, zeta potential measurements of the C50 composite were carried out. The pH values of the C50 suspensions were adjusted to 3.0, 7.0 and 11.0 using 1.0 M NaOH and 1.0 M HCl, respectively. It is seen that for all three pH values

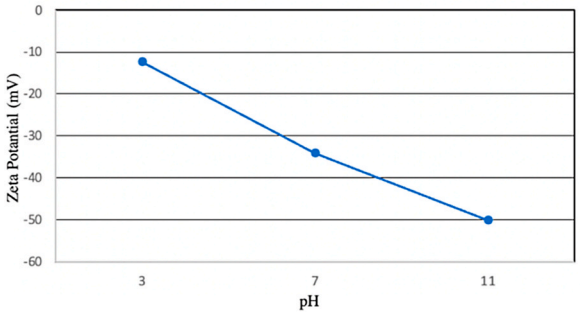

Fig. 5. Zeta potential measurements of the C50.

used in the experimental design, the composite surface is negatively charged and its magnitude increases as the pH value increases [31]. In a study where the zeta potential of the TiO_2 anatase phase was measured, it was observed that the zeta potential value decreased as the pH value increased [32]. In another study conducted for PS, it was reported that the zeta potential was adversely affected by the increase in pH value, similar to TiO_2 [33]. Considering the results in this study, the zeta potential behavior of the C50 composite containing PS and TiO_2 is also compatible with these studies in the literature [31–33].

3.6. Experimental design and optimization studies

The experimental design results according to were presented in Table 2 with the experimental measurement results and their predicted values. The minimum and maximum values of ciprofloxacin removal percentage were found to be 27 (R1) and 95 (R14), respectively. The results of the ANOVA test were shown in Table 3. After eliminating insignificant terms (p-value>0.05) from the model, the mathematical expression for the percent ciprofloxacin removal is as follows by Equation (2).

$$Y = 58,29\text{-}(10,5 * A)\text{-}(20,62 * B)\text{-}(8,37 * C) + (7,09 * B * B)\text{-}(5 * A * B)\text{-}(10 * A * C) \quad (2)$$

The R^2 value and the adjusted R^2 value were found to be 97.51 % and 95.65 %, respectively, ensuring the integrity of data.

According to Table 3, the p value of the model is less than 0.05 and the p value calculated for the lack-of-fit is greater than 0.05 ($F = 3.38$, $p = 0.246$) indicates that the significance level of the model is acceptable.

The effect of independent variables on the CIP removal were presented by contour plots in Fig. 6. As seen in Fig. 6a, the change in polymer content in the composite did not make a significant difference for constant pH values, while the increase in pH value caused a significant decrease in drug removal in the case of constant polymer content. The highest removal result was achieved with the composite with low pH value and medium polymer content. pH was observed as the most dominant factor. The fact that the coefficient of the B term in the model equation is higher than the coefficients of the other parameters and the p value of the term was obtained as <0.05 confirmed this situation (Table 3). It can be seen from Fig. 6b that at lower drug concentrations, the effect of polymer content was reduced compared to higher drug concentrations. Fig. 6c shows that the CIP initial concentration factor does not make a significant difference for constant pH. The elimination of the B*C term in the model equation is consistent with this result.

Table 2
Box-Behnken experimental design points and responses with their experimental and predicted values.

Runs	Independent Variables			Dependent Variables	
	A	B	C	Y (experimental)	Y(predicted)
R1	80	7	15	27	29
R2	50	7	10	59	58
R3	20	7	15	69	70
R4	50	7	10	57	58
R5	20	11	10	60	60
R6	20	3	10	90	91
R7	20	7	5	72	67
R8	80	7	5	70	66
R9	80	11	10	30	29
R10	80	3	10	80	80
R11	50	11	15	42	36
R12	50	11	5	47	53
R13	50	3	15	79	78
R14	50	3	5	95	94
R15	50	7	10	55	58

A = Amount of polymer (in composite, % by weight); B = pH; C= Ciprofloxacin initial concentration (mg/L); Y= Ciprofloxacin removal (%).

Table 3
ANOVA results for Box-Behnken experimental design.

Source	DF	Adj SS	Adj MS	F-Value	P-Value
Model	6	5533.88	922.31	52.31	0.000
Linear	3	4846.25	1615.42	91.62	0.000
A	1	882.00	882.00	50.02	0.000
B	1	3403.13	3403.13	193.01	0.000
C	1	561.13	561.13	31.82	0.000
Square	1	187.63	187.63	10.64	0.011
B*B	1	187.63	187.63	10.64	0.011
2-Way Interaction	2	500.00	250.00	14.18	0.002
A*B	1	100.00	100	5.67	0.044
A*C	1	400.00	400	22.69	0.001
Error	8	141.05	17.63		
Lack-of-fit	6	128.39	21.40	3.38	0.246
Pure Error	2	12.67	6.33		
Total	14	5674.93			

A = Amount of polymer (in composite, % by weight); B = pH; C= Ciprofloxacin initial concentration (mg/L); Y= Ciprofloxacin removal (%).

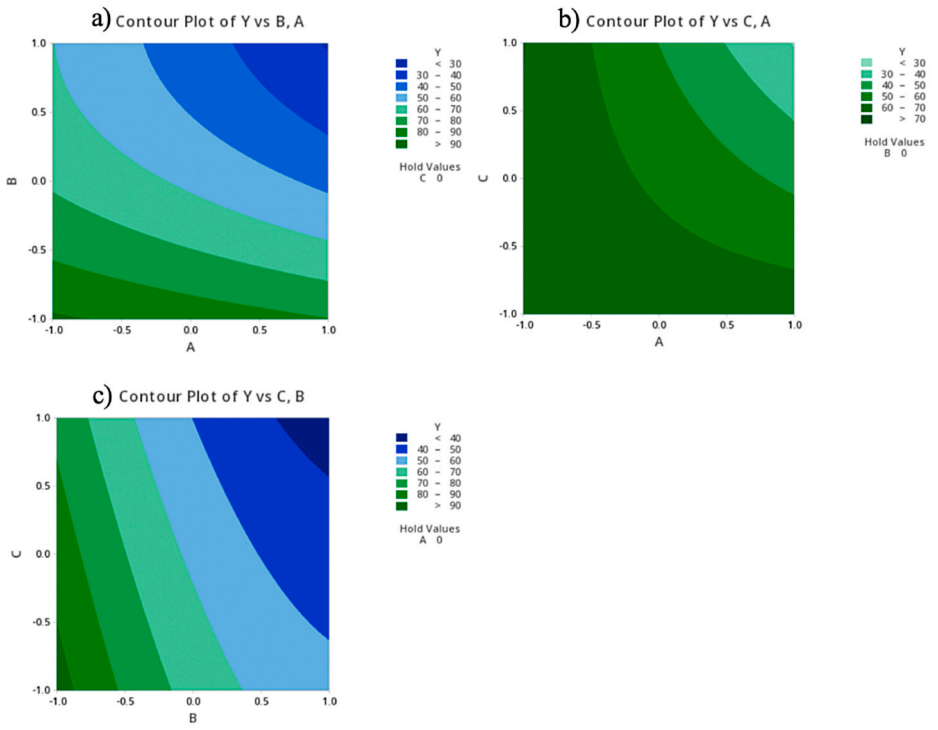

Fig. 6. Contour plots of CIP removal parameters showing the effect of independent variables (A = Amount of polymer (in composite, wt.%); B = pH; C= Ciprofloxacin initial concentration (mg/L); Y= Ciprofloxacin removal (%)).

3.7. Effect of polymer amount in composite

It is the TiO_2 content that shows the main photocatalytic effect in composites prepared using PS and TiO_2. In this study, photocatalytic degradation of composites with different TiO_2 and thus PS contents was investigated. Experimental design results showed that the removal performance deteriorated with increasing PS content. Since the amount of composite used in the experiments is the same, an increase in the polymer ratio means a decrease in TiO_2, which is the catalyst effect in the composite. The decrease in the amount of PS, that is, the increase in the amount of TiO_2, causes an increase in the production rate of the electron/hole pair and accordingly the hydroxyl radicals. This increase contributes to the improvement of photocatalytic degradation performance [20].

3.8. Effect of pH

When the experimental design results are evaluated, it is seen that the most influential parameter on the process is pH. The pH

change significantly affects the solution chemistry and, accordingly, the surface charge of the catalyst and the degree of ionization. Accordingly, the interactions between the catalyst surface, charged radicals and solvent molecules also change. It mainly affects the formation of hydroxyl radicals.

Due to a carboxyl group and an amine group in the CIP structure, it has two pK_A values of 6.1 and 8.7, respectively. Therefore, its solubility and hydrophobicity in water depend on pH. The solubility decreases as the pH increases. Below the value of $pK_{A1} = 6.1$, it is found in cationic form, while above the value of $pK_{A2} = 8.7$ it is in the anionic form. Between these two values, it exists in the zwitterionic form [3,34,35].

Likewise, when the zeta potential values of C50 are examined, it is seen that it changes depending on the pH. It is seen from the results of the zeta potential that the composite surface is negatively charged for each pH value (3,7 and 11) where the experiments are carried out, but the surface charge density increases as the pH increases.

It is thought that the reason for the dependence on pH in the removal process of CIP may be both the different speciation of CIP depending on pH and the changes in the surface charge density of the C50 composite. At pH 3, electrostatic attraction occurs because the cationic CIP and the composite surface are oppositely charged. At this pH, the adsorption of CIP is facilitated, thereby improving photocatalytic degradation. When the pH reaches 7, cationic groups leave their place to the zwitterionic structure, according to the first situation. Here the resolution of the CIP is also reduced. For these reasons, the interactions between the composite and CIP decrease, and accordingly, the removal performance at this pH worsens. Anionic CIP increases at pH = 11. At this pH value, the surface of the composite is also negatively charged. In other words, the removal process was adversely affected due to electrostatic repulsion between the negatively charged surface composite and the anionic CIP. Similar results are also found in the literature. For the aforementioned reasons, pH = 3 was chosen as the optimum pH value [3,34,35].

3.9. Effect of initial concentration

The initial drug concentration is one of the important parameters affecting the process. In order to examine its effect, it was chosen as a parameter in the experimental design and worked as 5,10 and 15 mg/L. When the experimental design results are evaluated, it is seen that the degradation efficiency decreases as the initial drug concentration increases. There are many possible reasons for this situation. One is that increasing concentration shortens the photon path entering the solution, resulting in lower photon adsorption on the catalyst particles. For this reason, the formation of hydroxyl radicals decreases and the photodegradation efficiency decreases. On the other hand, the probability of reaction increases as the concentration decreases. While the active sites on the photocatalyst surface can easily interact with the few CIP molecules in the medium, otherwise, only a part of the CIP can interact with the surface due to the excess in the medium with an increase in concentration. Thus, increasing the concentration decreases the degradation efficiency [3,34]. As expected due to the reasons mentioned above, the best removal result was obtained at the lowest drug concentration studied.

3.10. Effect of catalyst dosage

Catalyst dosage is also one of the important parameters in the photocatalytic degradation process. In this study, the effect of dosage was not selected separately as a parameter for the experimental design, but experiments were carried out with different catalyst dosages for the optimum conditions determined from the experimental design. Percentages of CIP removal against different catalyst dosages (20 mg, 30 mg, 40 mg and 50 mg) for the same amount of solution (50 ml solution is used in the experiments) are given in Fig. 7. While the photocatalytic degradation efficiency increased with the increase of the catalyst dosage up to a certain value, it decreased after a certain value.

The reason for this increase in the beginning is that the increase in the amount of catalyst increases the number of active sites in the environment and leads to an increase in the radicals that cause degradation. Despite that; when used above the critical amount of catalyst, turbidity occurs in the solution, which blocks UV radiation and reduces degradation performance. Another reason is that catalyst particles at high dosages undergo agglomeration during photodegradation. Due to agglomeration, the surface area is reduced

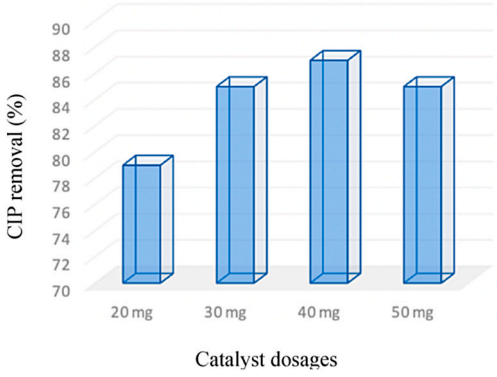

Fig. 7. CIP removal for different catalyst dosages.

and the drug removal performance is adversely affected [34,36,37].

3.11. Photocatalytic degredation kinetic

The photocatalytic degradation kinetics of CIP was investigated. For this purpose, the Langmuir-Hinshelwood model was used. Langmuir-Hinshelwood is one of the most widely used kinetic models in catalyst studies [38]. In photocatalytic degradation studies with TiO_2-containing catalyst, it has been reported that the process conforms to the L-H kinetic model [3,39–41]. In these studies, the formation or attack of hydroxyl radicals is generally considered as a rate limiting step. In addition, adsorption has a significant effect. For this reason, it is suitable for the use of the L-H model [42].

The L-H model equation (Equation (3)) is given as follows:

$$-\frac{dC}{dt} = \frac{kKC}{1+KC} \tag{3}$$

C is the concentration at any time of the degradation; t, illumination time; k is the reaction rate and K is the adsorption equilibrium coefficient.

There are two possibilities in such a process. The first possibility is working with dilute solutions. In this case, $KC \ll 1$ is assumed.

In condition $KC \ll 1$ (usually valid if C is in the range of ppb and a few ppm), Equation becomes pseudo first order kinetic [38,39,43,44] and Equation (3) can be written as follows:

$$In\left(\frac{C_0}{C}\right) = kKt = k_{app}t \tag{4}$$

Here (Equation (4)) k_{app} is pseudo first order rate constant (apparent rate constant). This rate constant is equal to the slope of the straight line when graphed $In\left(\frac{C_0}{C}\right)$ versus time.

The second possibility is when working at high concentration (Equation (5)), where $KC \gg 1$ is valid and Equation (3) becomes:

$$(C_0 - C) = k_{app}\ t \tag{5}$$

The graphs according to Equation (4) and Equation (5) of the experiments performed with different initial drug concentrations at constant pH using the same composite are given in Fig. 8(a–d). The R^2 values to be used in the evaluation of the fit with the kinetic model are also placed in the graphics. When the kinetic graphs of the experiment, which was carried out using 5 mg/L drug, are examined, it is seen that the R^2 value of the pseudo first order model is higher than the R^2 value of the zero-order model. In other words, it can be said that the results of 5 mg/L (dilute solution) fit the pseudo first order model as expected. The results of the experiments carried out using 15 mg/L are similar. However, when the R^2 values of the zero-order model graphs of both different initial concentrations are examined, it is seen that the R^2 value of the process with higher concentration (15 mg/L) is higher than the R^2 value of the process with lower concentration (5 mg/L). This is thought to be caused by an increase in the initial concentration. The results are consistent with the literature information [3,37–39].

The reaction kinetic graphs of the experiments performed with composites with the same initial concentration and pH value but with different polymer content are given in Fig. 9(a–d). As can be seen from the graphs of both composites, the process complied with the pseudo first order kinetics. As is known, the slope of the model equations given in these graphs is used to calculate the k_{app} value. Looking at these graphs, the k_{app} values of C20 and C80 composites are 0.011 min^{-1} and 0.007min^{-1}, respectively. Considering the experimental design results, it was determined that the removal performance decreased with the increase of the polymer content in the composites. Here, it is seen that the rate constant value of the composite with high polymer content is lower than the composite with low polymer content. This can explain that the reaction takes place more slowly in the composite with high polymer content, and therefore there is less removal in the same reaction time. These results are consistent with the results described in section 3.7.

4. Conclusions

In this study, composites were successfully synthesized using waste PS and TiO_2 at different ratios (C20, C50 and C80). This has been confirmed by XRD, FTIR, SEM and EDAX analysis. The usage of these composites as photocatalysts in the removal of CIP from wastewater by photocatalytic degradation was investigated. The effect of the polymer amount in the composite, pH and initial CIP concentration parameters on the removal process was observed. Box Behnken design, one of the experimental design methods, was used to examine the effect of these parameters. According to the experimental design results, it was understood that the most effective parameter on the process was pH and the optimum pH was pH = 3. At the same time, the most suitable composite for the process was selected as C50 composite with 50 % polymer content, while an initial CIP concentration of 5 mg/L was found to be optimum. In the experiment carried out under these conditions, maximum removal performance of 95 % was achieved. As a result of the experimental design, the model equation was obtained and the accuracy of the model was examined. It is seen that the estimated data obtained using the model equation and the results of the experimental trials are quite close to each other. In addition, the R^2, adjusted R^2 values of the model were 97.51 %, 95.65 %, respectively, and the p value was <0.05 indicating that the model represents the process well. In addition to the experimental design, the optimum catalyst amount was determined as 40 mg. Additionally, kinetic studies were performed for the photodegradation of CIP. It has been determined that the photocatalytic degradation of CIP by the catalyst synthesized and used in this study fits well with the Langmuir-Hinshelwood pseudo first order kinetic expression, with a high regression

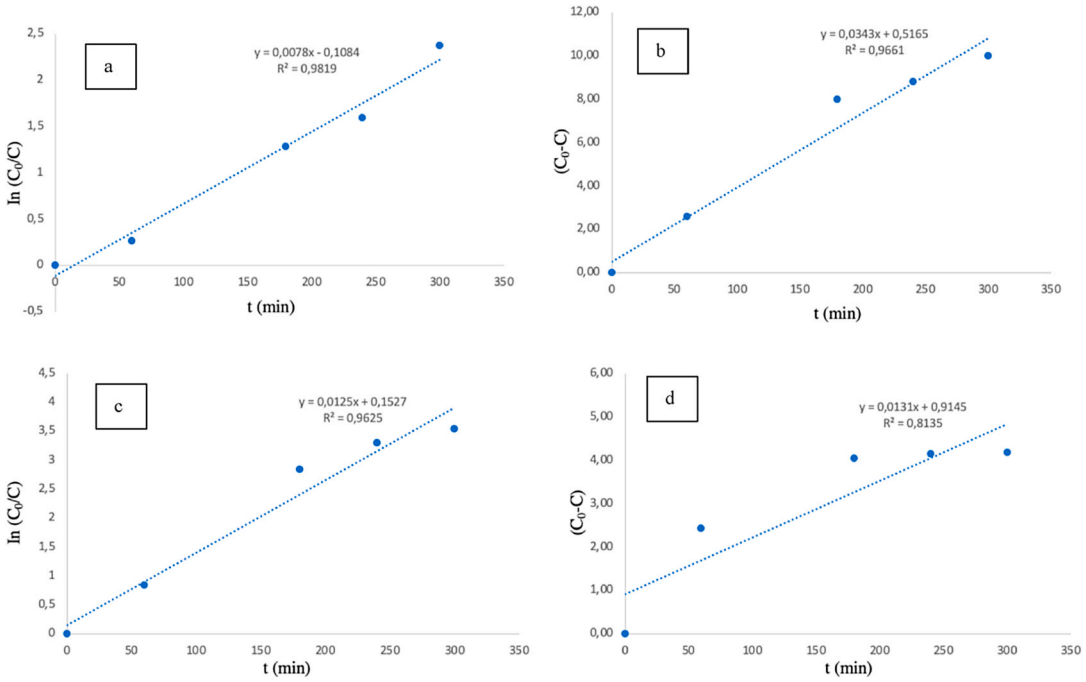

Fig. 8. L-H kinetic model plots for C50, a. Pseudo first order (conditions: 15 mg/L, pH = 3), b. Zero order (conditions: 15 mg/L, pH = 3), c. Pseudo first order (conditions: 5 mg/L, pH = 3) b. Zero order (conditions: 5 mg/L, pH = 3).

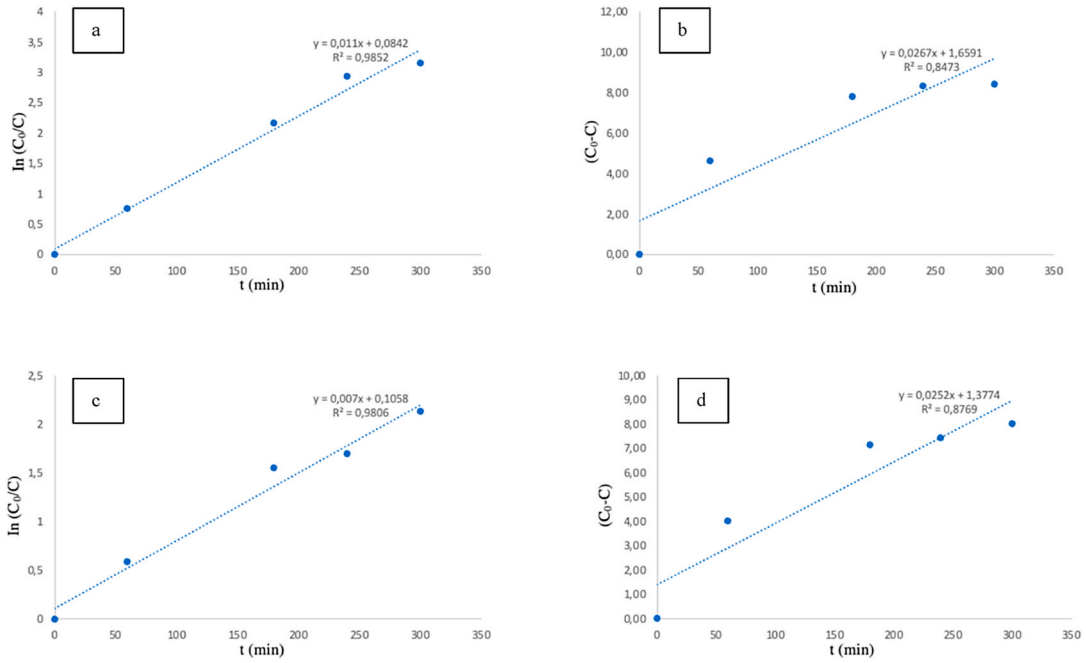

Fig. 9. L-H kinetic model plots for a. Pseudo first order (conditions: C20, 10 mg/L, pH = 3), b. Zero order (conditions: C20, 10 mg/L, pH = 3), c. Pseudo first order (conditions: C80, 10 mg/L, pH = 3) b. Zero order (conditions: C80, 10 mg/L, pH = 3).

value. In the light of these results, it was concluded that C50 could be successfully used as a catalyst for CIP removal. With the addition of PS, the difficulties encountered when TiO_2 was used alone were overcome, and a catalyst with similar or even higher performance (at relatively low drug concentrations) was synthesized using less TiO_2. On the other hand, it is of great importance that wastes are recycled and reused according to the circular economy. In this study, plastic spoon waste, which is frequently encountered and difficult

to dispose of, has been transformed into a new product and reused. In this context, a contribution was made to the circular economy by using one waste to clean another waste.

CRediT authorship contribution statement

Tugba Hayri-Senel: Writing – original draft, Validation, Methodology, Investigation, Formal analysis. **Ebru Kahraman:** Writing – review & editing, Validation, Methodology, Investigation, Formal analysis. **Serhat Sezer:** Writing – review & editing, Validation, Methodology, Investigation, Formal analysis. **Nalan Erdol-Aydin:** Resources, Investigation. **Gulhayat Nasun-Saygili:** Writing – review & editing, Supervision, Resources, Methodology.

Declaration of competing interest

The authors declare that they have no known competing financial interests or personal relationships that could have appeared to influence the work reported in this paper.

Acknowledgements

This study was supported by Istanbul Technical University Scientific Research Projects Unit (Grant: MGA-2021-43402).

References

[1] S. Shehu Imam, R. Adnan, N.H. Mohd Kaus, Photocatalytic degradation of ciprofloxacin in aqueous media: a short review, Toxicol. Environ. Chem. 100 (2018) 518–539, https://doi.org/10.1080/02772248.2018.1545128.
[2] P. Martins, S. Kappert, H.N. Le, V. Sebastian, K. Kühn, M. Alves, L. Pereira, G. Cuniberti, M. Melle-Franco, S. Lanceros-Méndez, Enhanced photocatalytic activity of au/TiO2 nanoparticles against ciprofloxacin, Catalysts 10 (2020), https://doi.org/10.3390/catal10020234.
[3] M. Malakootian, A. Nasiri, M. Amiri Gharaghani, Photocatalytic degradation of ciprofloxacin antibiotic by TiO2 nanoparticles immobilized on a glass plate, Chem. Eng. Commun. 207 (2020) 56–72, https://doi.org/10.1080/00986445.2019.1573168.
[4] T. Suwannaruang, J.P. Hildebrand, D.H. Taffa, M. Wark, K. Kamonsuangkasem, P. Chirawatkul, K. Wantala, Visible light-induced degradation of antibiotic ciprofloxacin over Fe–N–TiO2 mesoporous photocatalyst with anatase/rutile/brookite nanocrystal mixture, J. Photochem. Photobiol. Chem. 391 (2020), https://doi.org/10.1016/j.jphotochem.2020.112371.
[5] W. Li, Y. Zuo, L. Jiang, D. Yao, Z. Chen, G. He, H. Chen, Bi2Ti2O7/TiO2/RGO composite for the simulated sunlight-driven photocatalytic degradation of ciprofloxacin, Mater. Chem. Phys. 256 (2020), https://doi.org/10.1016/j.matchemphys.2020.123650.
[6] P.Y. Motlagh, S. Akay, B. Kayan, A. Khataee, Ultrasonic assisted photocatalytic process for degradation of ciprofloxacin using TiO2-Pd nanocomposite immobilized on pumice stone, J. Ind. Eng. Chem. 104 (2021) 582–591, https://doi.org/10.1016/j.jiec.2021.09.007.
[7] M. Shi, W. Li, Q. Wang, H. Xu, Y. Zhao, G. He, Q. Meng, H. Chen, One-step hydrothermal synthesis of BiVO4/TiO2/RGO composite with effective photocatalytic performance for the degradation of ciprofloxacin, Opt. Mater. 122 (2021), https://doi.org/10.1016/j.optmat.2021.111726.
[8] M. Chen, K. Zhuang, J. Sui, C. Sun, Y. Song, N. Jin, Hydrodynamic cavitation-enhanced photocatalytic activity of P-doped TiO2 for degradation of ciprofloxacin: synergetic effect and mechanism, Ultrason. Sonochem. 92 (2023), https://doi.org/10.1016/j.ultsonch.2022.106265.
[9] A. Hassani, A. Khataee, S. Karaca, Photocatalytic degradation of ciprofloxacin by synthesized TiO2 nanoparticles on montmorillonite: effect of operation parameters and artificial neural network modeling, J. Mol. Catal. Chem. 409 (2015) 149–161, https://doi.org/10.1016/j.molcata.2015.08.020.
[10] N. Parmar, J.K. Srivastava, Process optimization and kinetics study for photocatalytic ciprofloxacin degradation using TiO2 nanoparticle: a comparative study of Artificial Neural Network and Surface Response Methodology, J. Indian Chem. Soc. 99 (2022), https://doi.org/10.1016/j.jics.2022.100584.
[11] S. Krishnan, A. Shriwastav, Chlorophyll sensitized and salicylic acid functionalized TiO2 nanoparticles as a stable and efficient catalyst for the photocatalytic degradation of ciprofloxacin with visible light, Environ. Res. 216 (2023), https://doi.org/10.1016/j.envres.2022.114568.
[12] X. Hu, X. Hu, Q. Peng, L. Zhou, X. Tan, L. Jiang, C. Tang, H. Wang, S. Liu, Y. Wang, Z. Ning, Mechanisms underlying the photocatalytic degradation pathway of ciprofloxacin with heterogeneous TiO2, Chem. Eng. J. 380 (2020), https://doi.org/10.1016/j.cej.2019.122366.
[13] S. Singh, H. Mahalingam, P.K. Singh, Polymer-supported titanium dioxide photocatalysts for environmental remediation: a review, Appl. Catal. Gen. (2013) 462–463, https://doi.org/10.1016/j.apcata.2013.04.039, 178–195.
[14] M. Chen, K. Zhuang, J. Sui, C. Sun, Y. Song, N. Jin, Hydrodynamic cavitation-enhanced photocatalytic activity of P-doped TiO2 for degradation of ciprofloxacin: synergetic effect and mechanism, Ultrason. Sonochem. 92 (2023) 106265, https://doi.org/10.1016/j.ultsonch.2022.106265.
[15] X. Hu, X. Hu, Q. Peng, L. Zhou, X. Tan, L. Jiang, C. Tang, H. Wang, S. Liu, Y. Wang, Z. Ning, Mechanisms underlying the photocatalytic degradation pathway of ciprofloxacin with heterogeneous TiO2, Chem. Eng. J. 380 (2020) 122366, https://doi.org/10.1016/j.cej.2019.122366.
[16] I. Altin, M. Sökmen, Preparation of TiO2-polystyrene photocatalyst from waste material and its usability for removal of various pollutants, Appl. Catal., B 144 (2014) 694–701, https://doi.org/10.1016/j.apcatb.2013.06.014.
[17] S. Das, H. Mahalingam, Dye degradation studies using immobilized pristine and waste polystyrene-TiO2/rGO/g-C3N4 nanocomposite photocatalytic film in a novel airlift reactor under solar light, J. Environ. Chem. Eng. 7 (2019), https://doi.org/10.1016/j.jece.2019.103289.
[18] J. Shang, M. Chai, Y. Zhu, Solid-phase photocatalytic degradation of polystyrene plastic with TiO2 as photocatalyst, J. Solid State Chem. 174 (2003) 104–110, https://doi.org/10.1016/S0022-4596(03)00183-X.
[19] I. Salehi, M. Shirani, A. Semnani, M. Hassani, S. Habibollahi, Comparative study between response surface methodology and artificial neural network for adsorption of crystal violet on magnetic activated carbon, Arab J Sci Eng 41 (2016) 2611–2621, https://doi.org/10.1007/s13369-016-2109-3.
[20] S. Das, H. Mahalingam, Reusable floating polymer nanocomposite photocatalyst for the efficient treatment of dye wastewaters under scaled-up conditions in batch and recirculation modes, J. Chem. Technol. Biotechnol. 94 (2019) 2597–2608, https://doi.org/10.1002/jctb.6069.
[21] P. Srinivasu, S.P. Singh, A. Islam, L. Han, Novel approach for the synthesis of nanocrystalline anatase titania and their photovoltaic application, Adv. Optoelectron. (2011), https://doi.org/10.1155/2011/539382, 2011.
[22] J. Wang, J. Yu, X. Zhu, X.Z. Kong, Preparation of hollow TiO2 nanoparticles through TiO2 deposition on polystyrene latex particles and characterizations of their structure and photocatalytic activity, Nanoscale Res. Lett. 7 (2012), https://doi.org/10.1186/1556-276X-7-646.
[23] A.D. Acharya, B. Sarwan, R. Sharma, S.B. Shrivastava, M.K. Rathore, Study of interfaces in polymer-metal oxide films and free-volume hole using low-energy positron lifetime measurements, J. Sci.: Advanced Materials and Devices 4 (2019) 413–419, https://doi.org/10.1016/j.jsamd.2019.08.003.
[24] A.A. Ahmed, D.S. Ahmed, G.A. El-Hiti, M.H. Alotaibi, H. Hashim, E. Yousif, SEM morphological analysis of irradiated polystyrene film doped by a Schiff base containing a 1,2,4-triazole ring system, Appl Petrochem Res 9 (2019) 169–177, https://doi.org/10.1007/s13203-019-00235-6.
[25] S. Wanjale, M. Birajdar, J. Jog, R. Neppalli, V. Causin, J. Karger-Kocsis, J. Lee, P. Panzade, Surface tailored PS/TiO2 composite nanofiber membrane for copper removal from water, J. Colloid Interface Sci. 469 (2016) 31–37, https://doi.org/10.1016/j.jcis.2016.01.054.

[26] B. Jaleh, M.S. Madad, M.F. Tabrizi, S. Habibi, R. Golbedaghi, M.R. Keymanesh, UV-degradation effect on optical and surface properties of polystyrene-TiO2 nanocomposite film, J. Iran. Chem. Soc. 8 (2011), https://doi.org/10.1007/BF03254293. S161–S168.
[27] Z. Liu, Z. Jian, J. Fang, X. Xu, X. Zhu, S. Wu, Low-temperature reverse microemulsion synthesis, characterization, and photocatalytic performance of nanocrystalline titanium dioxide, Int. J. Photoenergy (2012) 1–8, https://doi.org/10.1155/2012/702503, 2012.
[28] G. Gohari, A. Mohammadi, A. Akbari, S. Panahirad, M.R. Dadpour, V. Fotopoulos, S. Kimura, Titanium dioxide nanoparticles (TiO2 NPs) promote growth and ameliorate salinity stress effects on essential oil profile and biochemical attributes of Dracocephalum moldavica, Sci. Rep. 10 (2020) 912, https://doi.org/10.1038/s41598-020-57794-1.
[29] S. Bagheri, K. Shameli, S.B. Abd Hamid, Synthesis and characterization of anatase titanium dioxide nanoparticles using egg white solution via sol-gel method, J. Chem. 2013 (2013), https://doi.org/10.1155/2013/848205, 1–5.
[30] M. Shahshojaei, H. Behniafar, M. Shaabanzadeh, Preparation and characterization of polystyrene/TiO_2 core-shell nanospheres via suspension technique, Adv Mat Res 829 (2013) 120–125. https://doi.org/10.4028/www.scientific.net/AMR.829.120.
[31] M.-S. Chun, H. Il Cho, I.K. Song, Electrokinetic behavior of membrane zeta potential during the filtration of colloidal suspensions, Desalination 148 (2002) 363–368, https://doi.org/10.1016/S0011-9164(02)00731-2.
[32] H. He, Y. Cheng, C. Yang, G. Zeng, C. Zhu, Z. Yan, Influences of anion concentration and valence on dispersion and aggregation of titanium dioxide nanoparticles in aqueous solutions, J. Environ. Sci. 54 (2017) 135–141, https://doi.org/10.1016/j.jes.2016.06.009.
[33] H. Xu, L.B. Casabianca, Probing driving forces for binding between nanoparticles and amino acids by saturation-transfer difference NMR, Sci. Rep. 10 (2020) 12351, https://doi.org/10.1038/s41598-020-69185-7.
[34] A. Hassani, A. Khataee, S. Karaca, Photocatalytic degradation of ciprofloxacin by synthesized TiO2 nanoparticles on montmorillonite: effect of operation parameters and artificial neural network modeling, J. Mol. Catal. Chem. 409 (2015) 149–161, https://doi.org/10.1016/j.molcata.2015.08.020.
[35] X. Li, W. Wang, J. Dou, J. Gao, S. Chen, X. Quan, H. Zhao, Dynamic adsorption of ciprofloxacin on carbon nanofibers: quantitative measurement by in situ fluorescence, J. Water Proc. Eng. 9 (2016), https://doi.org/10.1016/j.jwpe.2014.12.006 e14–e20.
[36] A. Kumar, A review on the factors affecting the photocatalytic degradation of hazardous materials, Material Science & Engineering International Journal 1 (2017), https://doi.org/10.15406/mseij.2017.01.00018.
[37] M.A. Rauf, S.S. Ashraf, Fundamental principles and application of heterogeneous photocatalytic degradation of dyes in solution, Chem. Eng. J. 151 (2009) 10–18, https://doi.org/10.1016/j.cej.2009.02.026.
[38] K.V. Kumar, K. Porkodi, F. Rocha, Langmuir–Hinshelwood kinetics – a theoretical study, Catal. Commun. 9 (2008) 82–84, https://doi.org/10.1016/j.catcom.2007.05.019.
[39] I. Konstantinou, Photocatalytic transformation of pesticides in aqueous titanium dioxide suspensions using artificial and solar light: intermediates and degradation pathways, Appl. Catal., B 42 (2003) 319–335, https://doi.org/10.1016/S0926-3373(02)00266-7.
[40] G.M. Neelgund, A. Oki, Photocatalytic activity of hydroxyapatite deposited graphene nanosheets under illumination to sunlight, Mater. Res. Bull. 146 (2022), https://doi.org/10.1016/j.materresbull.2021.111593.
[41] C. Mounir, H. Ahlafi, M. Aazza, H. Moussout, S. Mounir, Kinetics and Langmuir–Hinshelwood mechanism for the catalytic reduction of para-nitrophenol over Cu catalysts supported on chitin and chitosan biopolymers, React. Kinet. Mech. Catal. 134 (2021) 285–302, https://doi.org/10.1007/s11144-021-02066-w.
[42] O. Benhabiles, H. Mahmoudi, H. Lounici, M.F.A. Goosen, Effectiveness of a photocatalytic organic membrane for solar degradation of methylene blue pollutant, Desalination Water Treat. 57 (2016) 14067–14076, https://doi.org/10.1080/19443994.2015.1061954.
[43] A. Houas, H. Lachheb, M. Ksibi, E. Elaloui, C. Guillard, J.-M. Herrmann, Photocatalytic Degradation Pathway of Methylene Blue in Water, 2001.
[44] M. El-Kemary, H. El-Shamy, I. El-Mehasseb, Photocatalytic degradation of ciprofloxacin drug in water using ZnO nanoparticles, J. Lumin. 130 (2010) 2327–2331, https://doi.org/10.1016/j.jlumin.2010.07.013.